Proceedings of the
2007 IEEE Intelligent Vehicles Symposium
Istanbul, Turkey, June 13-15, 2007

Robust Yaw Stability Controller Design for a Light Commercial Vehicle Using a Hardware in the Loop Steering Test Rig

Sinan Oncu, Sertac Karaman, Levent Guvenc,
S.Server Ersolmaz, E.Serdar Ozturk, Emre Cetin, Mustafa Sinal

***Abstract*—This paper is on designing a multi-objective, robust parameter space steering controller for yaw stability improvement of a light commercial vehicle and its testing on a hardware-in-the-loop steering test rig. A linear single track model of the light commercial vehicle is used for controller design while its nonlinear version is used during hardware-in-the-loop simulations. The multi-objective design method used here maps *D*-stability, mixed sensitivity and phase margin bounds into the parameter space of chosen disturbance observer based steering controller filter parameters. The resulting controller design is tested using offline and hardware-in-the-loop simulations. A hardware-in-the-loop simulation test rig with the actual rack and pinion mechanism of the light commercial vehicle under study was built for this purpose. The steering control actuator is placed on the second pinion of the double pinion steering test system used. The hardware and geometry of the steering test rig are identical to the implementation of the steering system in the test vehicle. Unnecessary and expensive road testing is avoided with this approach as most problems are identified and solved in the hardware-in-the-loop simulation phase conducted in the laboratory where the steering subsystem and its controller exist as hardware and the rest of the vehicle being implemented exists as real time capable software. Hardware-in-the-loop simulation results show the effectiveness of the controller design proposed in this paper in tracking desired steering dynamics and in rejecting yaw disturbance moments.**

I. Introduction

DRIVER assistance systems based on active safety technology assist the driver in avoiding potentially hazardous situations by taking over control authority temporarily to provide corrective action during the panic reaction time of the driver. Yaw stability control of road vehicles is an important driver assistance system and is available commercially [1]. Yaw stability controllers are starting to become a standard like ABS as their benefit in helping the driver and avoiding accidents is better understood. Presently available commercial yaw stability controllers use differential braking technology as the ABS and traction control hardware is already available for implementation. Steering actuation based yaw stability control is also possible and is available commercially in the form of active steering where the mechanical linkage between the steering wheel and the steering rack is kept in place, but an electric steering actuator is used to complement the mechanical driver input. The highest benefit from steering actuated yaw stability control can be achieved when steer-by-wire technology is used. In a steer-by-wire system, there is no mechanical connection between the steering wheel and the steering rack. Currently, production vehicles with true steer-by-wire do not exist, even though the steer-by-wire solution has been available for some time. One reason for this unavailability is the fact that customers do not place a high demand for steer-by-wire at present.

The European Commission has set a goal of reducing road accident related fatalities by half by the year 2010. Yaw stability control will be a vital part of reaching such a goal along with other driver assistance systems. This paper is a continuation of earlier work by the authors reported in [2] and [3]. Reference [2] is on yaw stability control of a light commercial vehicle. Various models for the light commercial vehicle under study were presented in [2] and were shown to be in good agreement with its validated high fidelity model. The light commercial vehicle fitted with an active steering system was subjected to a limited number of yaw stability control and electric power assisted steering tests in [2] and [3]. Experience gained in the previous work reported in [2] and [3] have shown that the best approach to developing a steering control system for the light commercial vehicle under study is to do extensive testing and development in the laboratory using a hardware-in-the-loop test system before conducting road tests. This approach is motivated by several factors:

- Different electric motors can be tested easily in a laboratory hardware-in-the-loop setup as compared to retrofitting it in the test vehicle.
- It is possible to test conditions like icy road, μ-split braking etc. which are difficult and expensive in road testing.
- It is also possible to design test scenarios that may not be possible to achieve in a road test.
- It is possible to inject soft sensor and actuator failures in a hardware-in-the-loop simulation without having

Manuscript received January 30, 2007. The first three authors acknowledge support of the European Union Framework Programme 6 through the AUTOCOM SSA project (INCO Project No: 16426) and the support of Ford Otosan through project UG 03.016.

S. Oncu, S. Karaman, and L. Guvenc are with the Automotive Control and Mechatronics Research Center of Istanbul Technical University, Gumussuyu, Taksim, Istanbul, TR-34437, Turkey (corresponding author e-mail: oncusi@itu.edu.tr).

S.S. Ersolmaz, E. S. Ozturk, E. Cetin and M. Sinal are with Ford Otosan, TR-41670, Gölcük, Kocaeli, Turkey.

1-4244-1068-1/07/$25.00 ©2007 IEEE.

to worry about safety.

- It is possible to easily test different steering concepts like electric power assisted steering, active steering and steer-by-wire by making small changes to a modular steer-by-wire system.
- Researchers can concentrate only on the steering system including its actuators, sensors and controller as the rest of the system exists as software and cannot fail during the tests.

The organization of the rest of the paper is as follows. The linear and nonlinear single track models used for controller design, offline and real time simulations are presented in Section 2. The disturbance observer used as a steering controller in this paper is presented in Section 3. Results of the multi-objective design based on mapping *D*-stability, mixed sensitivity and phase margin bounds into the parameter space of disturbance observer based steering controller filter parameters is presented in Section 4. Details of the home built, modular hardware-in-the-loop test system developed for testing yaw stability controllers for a light commercial vehicle are given in Section 5. Offline and real time simulation results based on the hardware-in-the-loop system are the topic of Section 6. The paper ends with conclusions.

II. Vehicle Models Used

Two vehicle models are used in this paper. The first one is the classical linear single track vehicle model (see [4]) which is used for controller design. The second vehicle model is the nonlinear version of the single track vehicle model and is used in the simulations. Explanation of the symbols used can be found in Table 1.

The classical single track model geometry and its variables are illustrated graphically in Figure 1. The single track vehicle model captures the lateral dynamics of a road vehicle quite accurately in handling maneuvers where lateral acceleration does not exceed 0.3g. The

TABLE I
VEHICLE MODEL PARAMETERS

Symbol	Explanation
$F_f\ (F_r)$	Lateral wheel force at front (rear) wheel
M_{zd}	Yaw disturbance moment
r	Yaw rate
β	Chassis side slip angle at vehicle center of gravity
$\alpha_f\ (\alpha_r)$	Front (rear) tire side slip angle
v	Vehicle speed at center of gravity point
$l_f\ (l_r)$	Distance from front (rear) axle to center of gravity
δ_f	Front wheel steering angle
m	The mass of the vehicle
I_z	The moment of inertia w.r.t. a vertical axis through the center of gravity
$c_f\ (c_r)$	Front (rear) wheel cornering stiffness
μ	Road friction coefficient

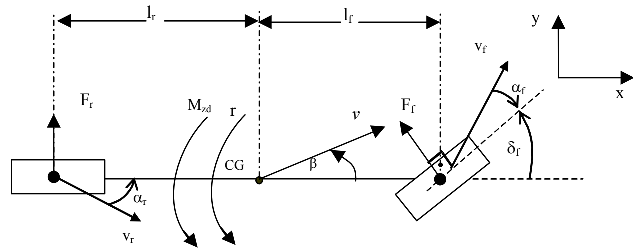

Fig. 1. Geometry of the single track vehicle model

nonlinear single track model is characterized by the force coordinate transformation due to steering angle projection given by

$$\begin{bmatrix} \sum F_x \\ \sum F_y \\ \sum M_z \end{bmatrix} = \begin{bmatrix} -\sin\delta_f & -\sin\delta_r \\ \cos\delta_f & \cos\delta_r \\ l_f\cos\delta_f & -l_r\cos\delta_r \end{bmatrix} \begin{bmatrix} F_f \\ F_r \end{bmatrix}, \tag{1}$$

the dynamics equations

$$\begin{bmatrix} mv(\dot\beta + r) \\ m\dot v \\ I_z\dot r \end{bmatrix} = \begin{bmatrix} -\sin\beta & \cos\beta & 0 \\ \cos\beta & \sin\beta & 0 \\ 0 & 0 & 1 \end{bmatrix} \begin{bmatrix} \sum F_x \\ \sum F_y \\ \sum M_z \end{bmatrix}, \tag{2}$$

and the equations of kinematics/geometry

$$\tan\beta_f = \tan\beta + \frac{l_f r}{v\cos\beta}, \tag{3}$$

$$\tan\beta_r = \tan\beta - \frac{l_r r}{v\cos\beta}. \tag{4}$$

The tire longitudinal forces F_f and F_r are nonlinear functions of the corresponding side slip angles α_f and α_r. F_f and F_r also depend on the friction characteristics between the road and the tires. The nonlinear single track model is illustrated in the top part of the block diagram of Figure 2 while its linearized version is shown in the bottom part of the same figure.

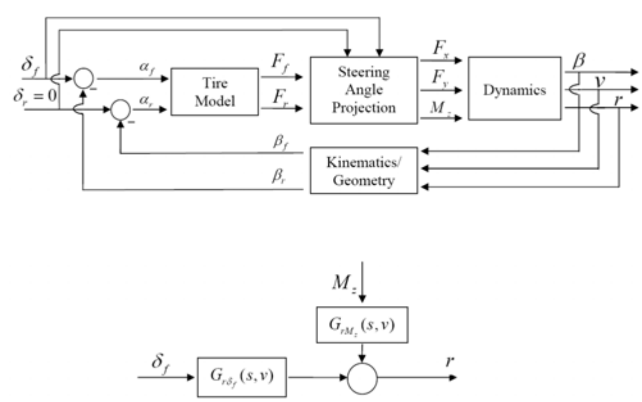

Fig. 2. Nonlinear (top) and linearized (bottom) single track model block diagrams

The nonlinear single track model is linearized assuming small steering angles δ_f and small side slip angle β. The tire force characteristics are linearized as

$$F_f(\alpha_f) = \mu C_{f0}\alpha_f = C_f\alpha_f\,,\quad F_r(\alpha_r) = \mu C_{r0}\alpha_r = C_r\alpha_r \tag{5}$$

with the tire cornering stiffnesses C_f, C_r the road-tire friction coefficient μ and the tire side slip angles given by

$$\alpha_f = \delta_f - \left(\beta + \frac{l_f}{v} r\right) \tag{6}$$

$$\alpha_r = -\left(\beta - \frac{l_r}{v} r\right) \tag{7}$$

Note that C_{f0} and C_{r0} in (5) are the nominal values for dry road ($\mu = \mu_n = 1$) of the tire cornering stiffnesses. The transfer function from the front wheel steering angle δ_f to the yaw rate r is given by

$$G_{r\delta_f}(s,v) = \frac{r(s)}{\delta_f(s)} = \frac{b_1(v)s + b_0(v)}{a_2(v)s^2 + a_1(v)s + a_0(v)} \tag{8}$$

with

$$b_0 = c_f c_r (l_f + l_r)v$$

$$b_1 = c_f l_f m v^2$$

$$a_0 = c_f c_r (l_f + l_r)^2 + (c_r l_r - c_f l_f) m v^2$$

$$a_1 = (c_f(I_z + l_f^2 m) + c_r(I_z + l_r^2 m))v$$

$$a_2 = I_z m v^2$$

$G_{r\delta f}(s,v)$ in (8) is also called the steering wheel input response transfer function here. The d.c. gain of the nominal single track model (8) is

$$K_n(v) = \lim_{s\to 0} G_{r\delta_f}(s,v)\Big|_{\mu=\mu_n=1} \tag{9}$$

at the chosen longitudinal speed v and for $\mu = \mu_n = 1$.
The yaw moment disturbance input response is given by

$$G_{rM_z}(s,v) = \frac{r(s)}{M_z(s)} = \frac{mv^2 s + (c_f + c_r)v}{a_2(v)s^2 + a_1(v)s + a_0(v)} \tag{10}$$

The block diagram of the linearized single track model is shown in the bottom of Figure 2.

III. Disturbance Observer Based Steering For Yaw Stability Control

The yaw stability controller used here is based on the disturbance observer architecture [5-9]. The block diagram of the disturbance observer based yaw stability controller is shown in Figure 3.

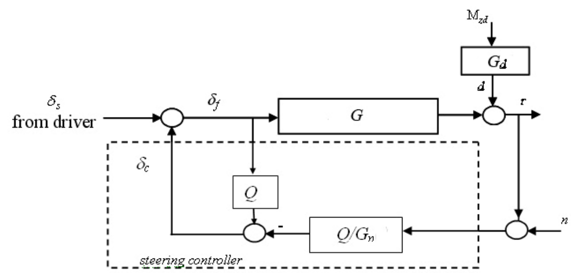

Fig. 3. Disturbance observer based yaw stability controller block diagram

The loop gain of the yaw stability controller compensated plant is $L = GQ/G_n(1-Q)$ with the steering model regulation, lateral disturbance rejection, and sensor noise rejection transfer functions being given by

$$\frac{r}{\delta_s} = \frac{G_n G}{G_n(1-Q) + GQ} \tag{11}$$

$$\frac{r}{M_d} = \frac{G_d}{1+L} \equiv G_d S = \frac{G_n(1-Q)G_d}{G_n(1-Q) + GQ} \tag{12}$$

$$\frac{r}{n} = \frac{-L}{1+L} \equiv -T = \frac{-GQ}{G_n(1-Q) + GQ} \tag{13}$$

In (12) and (13), S and T are the sensitivity and complementary sensitivity functions, respectively. The choice of Q as a low pass filter with unity d.c. gain results in $r/\delta_s \to G_n$ which is the desired steering dynamics (steering model regulation) and $r/M_{zd} \to 0$ (disturbance rejection) at low frequencies where $Q \to 1$. At higher frequencies where there may be considerable sensor noise, $r/n \to 0$ (sensor noise rejection) will be achieved as $Q \to 0$. This choice of $Q \to 0$ at higher frequencies is also necessitated by the robustness of stability requirement. Then, the input-output behavior of the controlled system including its steady-state behavior will be the same as that of the nominal (or desired) model G_n up to the bandwidth of the low pass filter Q (steering model regulation along with good disturbance rejection).

In this study, the Q filter was chosen to be the simple low pass filter

$$Q(s) = \frac{1}{\tau_Q s + 1} \tag{14}$$

The desired yaw dynamics model was chosen to be the first order system given by

$$G_n(s,v) = \frac{K_n(v)}{\tau_n s + 1} \tag{15}$$

In (15) $K_n(v)$ is the velocity scheduled single track model static gain. Two design parameters in the steering actuated disturbance observer are chosen as τ_Q in (14) and τ_n in (15). These two parameters form the controller parameter space used in design in the next section.

IV. Multi-Objective Parameter Space Design

The model parameters that vary the most and are, therefore, crucial for robustness are road-tire friction coefficient μ and the vehicle speed v. Figure 4 displays the region in the μ-v plane where yaw stability controller design objectives should be satisfied. Six representative design points marked with cross signs in Figure 4 are used in the design procedure.

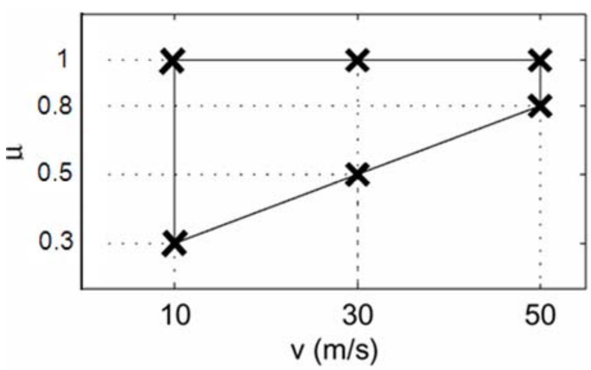

Fig. 4. Region of uncertain parameters

Different control objectives are evaluated at each of these representative points to obtain corresponding τ_n-τ_Q controller parameter space regions. Graphical intersection of all six solution regions in the τ_n-τ_Q parameter space results in the solution region where the chosen objective is satisfied at all six design points. Multi-objective design is achieved by graphically intersecting parameter space solution regions for each objective. Three objectives are chosen here. They are satisfaction of D-stability, mixed sensitivity and parameter space bounds.

A typical D-stability region is shown in Figure 5. The D-stability boundaries are formed by assuming roots no closer than 0.8 to the imaginary axis and no further than 7 from the imaginary axis. A maximum damping of 80 degrees corresponding to a damping ratio of $\xi = 0.17$ is also assumed for generating the solution regions. The D-stability regions corresponding to the six design points of Figure 4 are given in Figure 6 where the solution regions are shaded.

The overall solution region which combines all solution regions in Figure 6 is shown in Figure 7. The combined solution region in Figure 7 satisfies the D-stability criteria for all six design points.

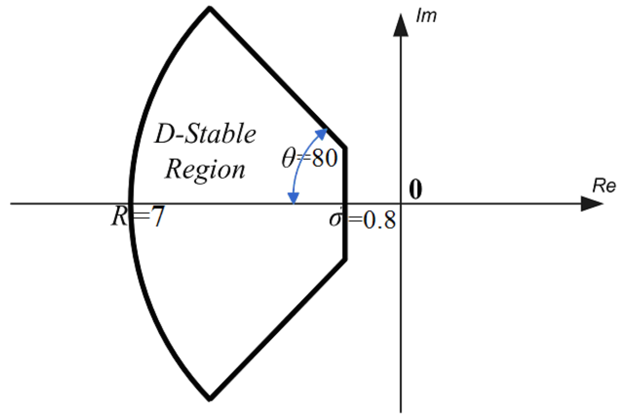

Fig. 5. D-stability region in the complex plane

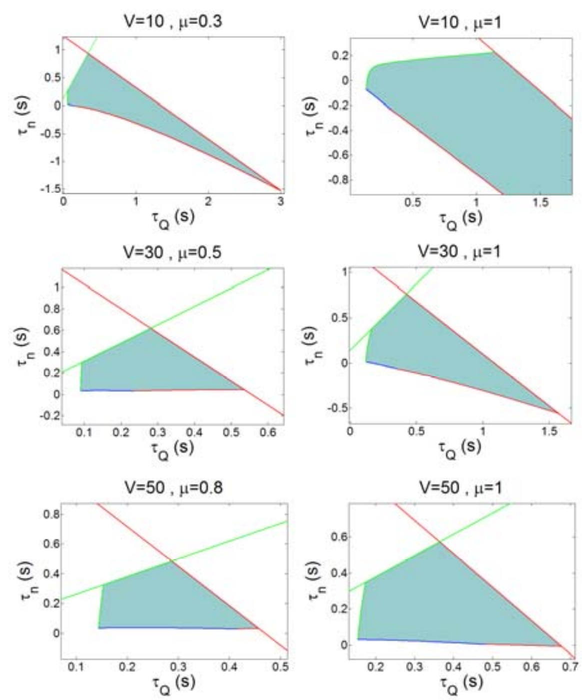

Fig. 6. *D*-stability regions for the six design points

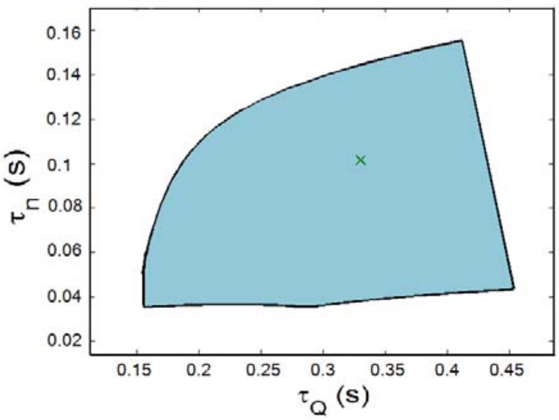

Fig.7. Overall *D*-stability region

A phase margin that is larger than 40° is the second objective that is chosen for the design. The combined solution region for the phase margin bound is shown as the shaded area in Figure 8.

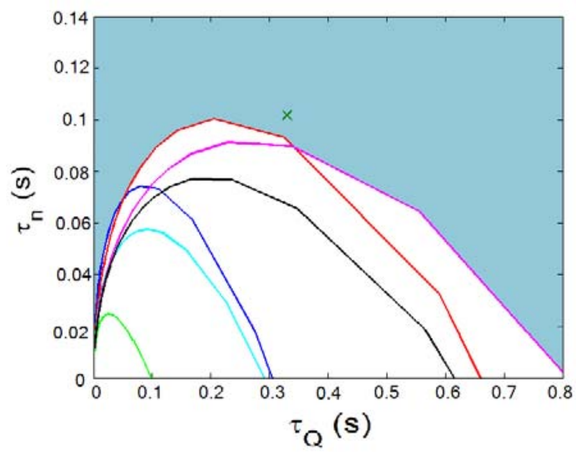

Fig.8. Phase margin bounds and combined solution area for six operating points

The third objective is to map a mixed sensitivity H_∞ norm bound

$$\left|W_s S\right| + \left|W_T T\right| < 1 \text{ for } \forall \omega \tag{16}$$

to the τ_n - τ_Q disturbance observer parameter space region [10]. The sensitivity weights in (16) are:

$$W_S^{-1} = h_S \frac{s+\omega_S l_S}{s+\omega_S h_S}, \quad W_T = h_T \frac{s+\omega_T l_T}{s+\omega_T l_T} \tag{17}$$

where $l_S = 0.5$, $h_S = 4$ and $\omega_S = 3$ rad/s are for the sensitivity transfer function and $l_T = 0.1$, $h_T = 1.5$ and $\omega_T = 20$ rad/s are for the complementary sensitivity transfer function. The mixed sensitivity solution regions are shown in Figure 9.

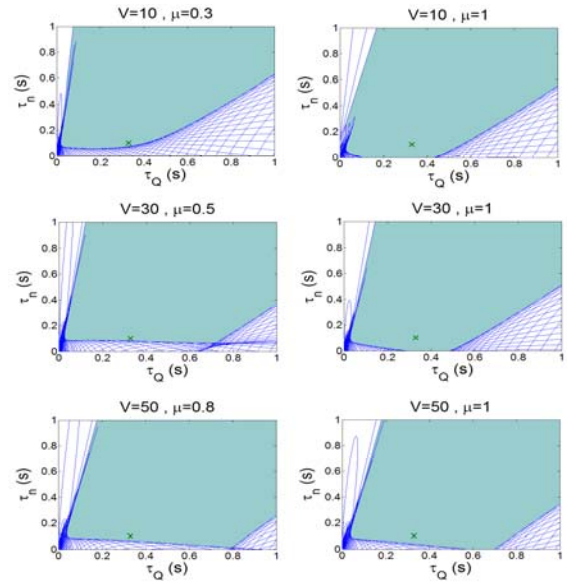

Fig.9. Mixed sensitivity solution regions for the six design points

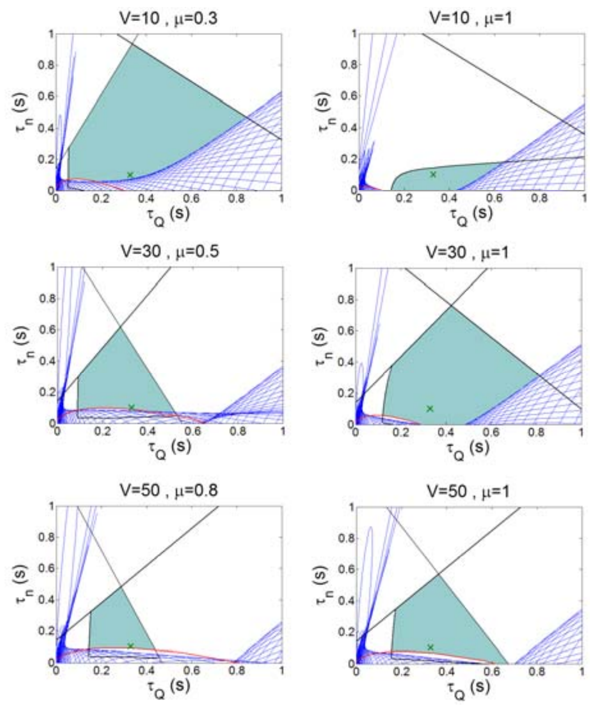

Fig.10. Combined solution regions for the six design points

The multi-objective solution regions of *D*-Stability, phase margin and mixed sensitivity bounds being mapped to the τ_n - τ_Q disturbance observer parameter space are shown for the six design points in Figure 10. The overall multi-objective design region formed by intersecting all regions in Figure 10 is displayed in Figure 11. The point marked with a cross (see also figures 6-10) shows the controller parameters that are chosen as the specific solution to be used in the offline and real time simulations of the next section.

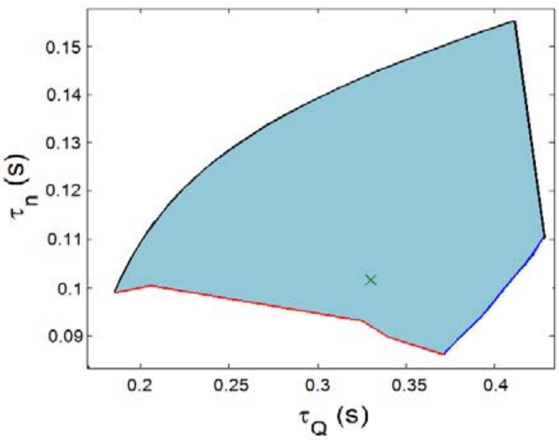

Fig.11. Overall multi-objective solution region

V. Hardware-in-The-Loop Test Setup

A modular steering test rig corresponding, in principal, to the steering subsystem of the Ford Transit Connect light commercial vehicle has been prepared as a hardware-in-the-loop testbed. The test rig shown in Figure 12 has a modular structure which makes it possible to be used in both active steering and steer-by-wire configurations. There are two electric motors mounted on the test rig at present, one brushless and one brush-type d.c. motor. The electric motors used can be changed easily.

Fig.12. Steering Test Rig

The electric motor actuators are utilized for different tasks depending on the steering actuation method. In the steer-by-wire configuration Figure 13 (top) the d.c. motor mounted on the second pinion is used as the steering actuator while the motor on the steering column provides the driver torque feedback. In the electric power assisted steering configuration, Figure 13 (bottom), the column motor provides the power assist to the driver while the motor on the second pinion is used to generate external disturbances and tire road forces in order to provide realistic driving conditions and to make controller performance examination possible. The setup can easily be converted from one configuration to the other by removing/mounting the mechanical connection between the steering column and the rack that is marked with “A” in Figure 13. It is also possible to use this setup to test a double pinion active steering configuration (see [1-2]).

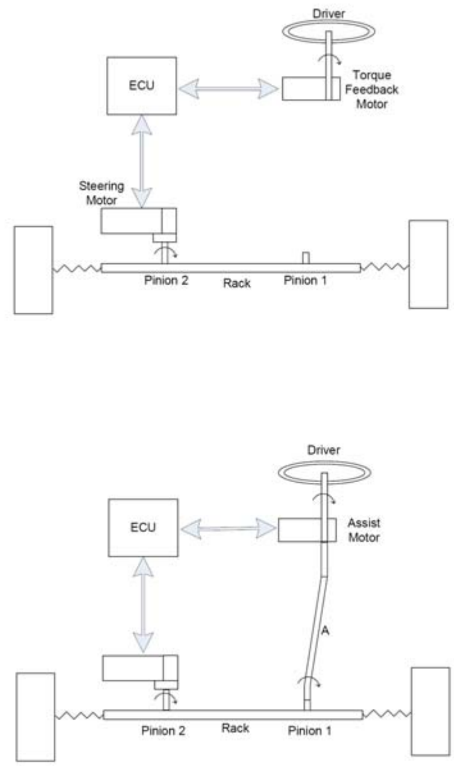

Fig.13. Different steering architectures that can be investigated using the steering test rig

In this paper, disturbance observer based vehicle yaw stabilization with steering actuation is realized through the steer-by-wire implementation. Figure 14 shows the schematic diagram of the hardware-in-the-loop setup used. Four types of simulations are used to assess the yaw stability controller performance, effect of actuator dynamics and hardware-in-the-loop performance. They are offline simulation without yaw stability control, offline simulation with yaw stability control, offline simulation with yaw stability control and an actuator dynamics model and hardware-in-the-loop simulation with yaw stability control.

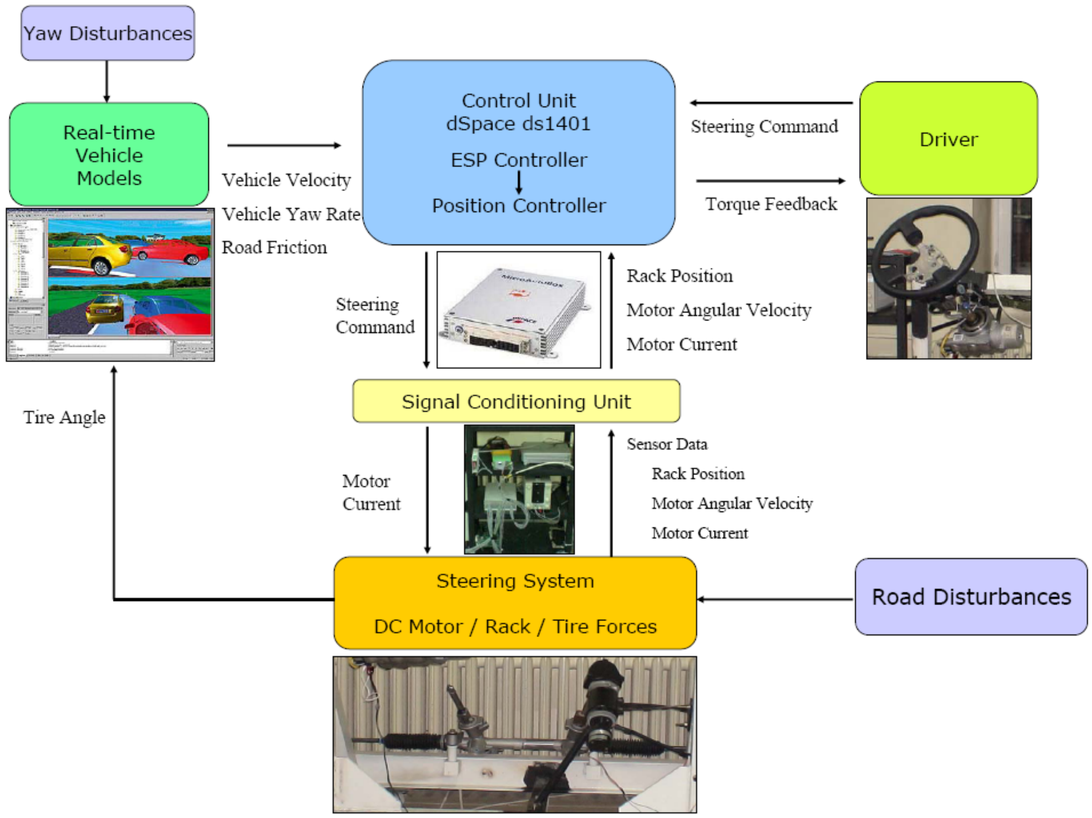

Fig.14. Schematic respresentation of steer-by-wire hardware-in-the-loop simulator components and their interactions

All four simulation types are subject to the same driving conditions, driver inputs and disturbances. In the hardware-in-the-loop simulations, vehicle dynamics are implemented as software that runs in real time. The yaw stability controller obtains the required vehicle dynamics information from the software model and commands the corrective steering actions to the actual steering actuator. The low level position controller of the steering system receives the steering command and drives the steering electric motor to bring the rack to the desired position. The rack position is converted to the corresponding tire angle by using a look up table. Yaw stabilization through steering actuation requires precise positioning of the tire angles. Therefore, a low-level position controller that utilizes a PD controller compensating the d.c. electric motor dynamics which is placed under another disturbance observer compensation, designed to realize steering commands issued by the yaw stability controller, is used. Details of this low level controller are not given here for the sake of brevity.

VI. Offline And Real-Time Simulation Results

An extensive simulation study was performed for all of the six design points. For the sake of brevity, only two results will be presented. The first hardware-in-the-loop simulation result shown in Figure 15 is the steering wheel step input response of the nonlinear single track vehicle model explained in Section 2 with three of the four different simulation types explained in the beginning of this section. In the second simulation in Figure 16, a step yaw moment disturbance was applied. The simulation results displayed in Figure 15 illustrate the satisfactory following of the desired steering step input while the results displayed in Figure 16 demonstrate excellent disturbance rejection. The steering actuator commanded by the yaw stability controller and the actual steering action output in the hardware-in-the-loop simulation are shown in Figure 17 during yaw moment disturbance rejection. Commanded and actual steering actions are seen to be almost identical.

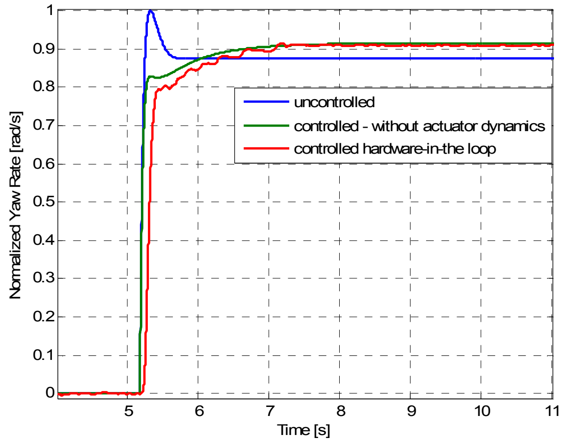

Fig.15. Step steering command input response simulation (normalized)

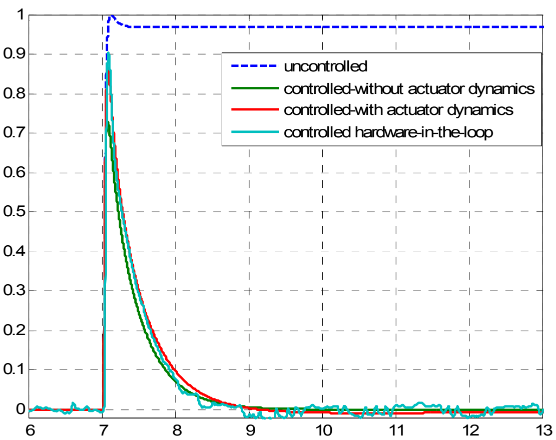

Fig. 16. Step yaw moment disturbance simulation (normalized)

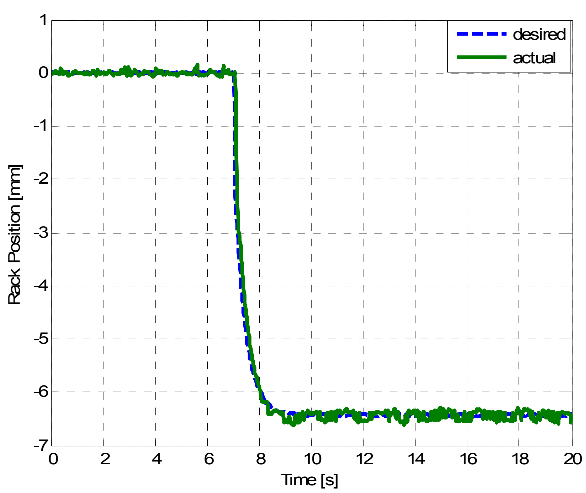

Fig.17. Commanded and actual (hardware-in-the-loop) steering actuator action

VII. Conclusions

A multi-objective design method was used to maps *D*-stability, mixed sensitivity and phase margin bounds into the parameter space of chosen disturbance observer based steering controller filter parameters. The resulting controller design was tested using offline and hardware-in-the-loop simulations. A hardware-in-the-loop simulation test rig with the actual rack and pinion mechanism of the light commercial vehicle under study was built for this purpose. Offline and hardware-in-the-loop simulation results showed the effectiveness of the controller design proposed in this paper in tracking desired steering dynamics and in rejecting undesired yaw disturbance moments.

References

[1] van Zanten, A.T., Erhardt, R. and Pfaff, G. (1995). VDC, the vehicle dynamics control system of Bosch. *SAE paper No. 950759.*

[2] Güvenç, L., Ersolmaz, Ş.S., Öncü, S., Öztürk, E.S., Çetin, E., Kılıç, N., Güngör, S., Kanbolat, A., 2006, "Stability Enhancement of a Light Commercial Vehicle Using Active Steering," SAE Paper No: 2006-01-1181, *SAE World Congress and Exhibition, Steering and Suspension Technology Symposium*, Detroit, 2006, April 3-6.

[3] Karaman, S., Öncü, S., Güvenç, L., Ersolmaz, Ş.S., Çetin, E., Kanbolat, A., 2006, "Robust Velocity Scheduled Yaw Stability Control of a Light Commercial Vehicle," *IEEE Intelligent Vehicles Symposium*, Tokyo, 2006, June 13-15.

[4] J. Ackermann, P. Blue, T. Bünte, L. Güvenç, D. Kaesbauer, M. Kordt, M. Muhler and D. Odenthal, *Robust Control: the Parameter Space Approach*. Springer-Verlag, 2002.

[5] Ohnishi, K. (1987). "A new servo method in mechatronics." *Trans. Japanese Soc. Elect. Eng.*, vol. 107-D, pp. 83-86.

[6] Umeno, T. and Hori, Y. (1991). "Robust speed control of dc servomotors using modern two degrees-of-freedom controller design." *IEEE Transactions on Industrial Electronics*, vol 38, no. 5, pp. 363-368.

[7] Aksun Güvenç, B., Bünte, T., Odenthal, D., Güvenç, L., 2004, "Robust Two Degree of Freedom Vehicle Steering Compensator Design," *IEEE Transactions on Control Systems Technology*, Vol. 12, no. 4, pp. 627-636, 2004.

[8] Aksun Güvenç, B., Güvenç, L., "The Limited Integrator Model Regulator and its Use in Vehicle Steering Control," *Turkish Journal of Engineering and Environmental Sciences*, pp. 473-482, 2002.

[9] Aksun Güvenç, B., Güvenç, L., "Robust Two degree of Freedom Add-On Controller Design for Automatic Steering," *IEEE Transactions on Control Systems Technology*, Vol. 10, no 1, pp. 137-148, 2002

[10] Güvenç, L., Ackermann, J., "Links Between the Parameter Space and Frequency Domain Methods of Robust Control," *International Journal of Robust and Nonlinear Control*, Vol. 11, no. 15, pp. 1435-1453, 2001.